

# MANGANESE PEBBLES FROM HOCHSCHARTEHÖHLESYSTEM (THE HOHER GÖLL MASSIF, AUSTRIA): INSIGHT INTO POTENTIAL GENESIS AND PROVENANCE

Ditta KICIŃSKA\* , Jacek MICHNIEWICZ & Michał KUBIAK

*Institute of Geology, Adam Mickiewicz University,  
Bogumiła Krygowskiego 12, 61-680 Poznań, Poland;  
e-mail: kicinska@amu.edu.pl, jacekm@amu.edu.pl, michal.kubiak@amu.edu.pl  
\* Corresponding author*

Kicińska, D., Michniewicz, J. & Kubiak, M., 2023. Manganese pebbles from Hochschartehöhlesystem (the Hoher Göll Massif, Austria): insight into potential genesis and provenance. *Annals Societatis Geologorum Poloniae*, 93: 211–223.

**Abstract:** Heavy, black manganese pebbles have been found in the clastic sediments of the Hochschartehöhlesystem (the Northern Calcareous Alps). Six selected pebbles were subjected to X-ray diffraction, optical microscopy and optical and electron microscopy analysis. The results reveal that the main component of the pebbles is manganese silicate, braunite,  $\text{Mn}^{2+}\text{Mn}^{3+}_6(\text{SiO}_4)_8$ . Braunite is a mineral formed at elevated temperatures, mainly through hydrothermal, metamorphic or diagenetic processes. This means that the manganese pebbles were formed outside the caves. However, manganese rock was not found *in situ* on the surface of the Hoher Göll Massif. This probably indicates that their origin is from eroded parts of Mesozoic rocks. The first studies of pebbles and their mineralogy, by analogy with contemporary marine sediments, indicate that their genesis is related to spreading zones and accompanies hydrothermal vents. The analysed material highlights two important issues: (1) the manganese pebbles are significant arguments for the occurrence of hydrothermal vents in the Northern Calcareous Alps; and (2) the importance of cave sediments studies, which provide relevant evidence for palaeogeographic reconstruction.

**Key words:** Northern Calcareous Alps, cave sediments, manganese pebbles, submarine vents, braunite.

*Manuscript received 30 July 2022, accepted 14 February 2023*

## INTRODUCTION

Cave clastic sediments are important clues in the reconstruction of the phases of cave evolution, palaeoflow directions, cave formation in relation to the geomorphic evolution of mountains, tectonic studies, and palaeoclimatic reconstruction (e.g., Bosák, 1989; Hercman, 2000; Ford and Williams, 2007; Sasowsky, 2007; Szczygieł *et al.*, 2020a, b; Bella *et al.*, 2021). Clastic material that enters caves can originate from faraway sources, both inside the massif and on the former surface with a different erosional surface than the recent one.

Manganese oxides represent a common deposit in karst caves and usually form coatings on cave walls (Hill and Forti, 1997; Ford and Williams, 2007; White *et al.*, 2009) in thicknesses of one to a few millimetres. In cave sediments, they are often accumulated in the form of manganese fluff (e.g., Boston, 2004) and could be soft (the so-called ‘wad’) or a consolidated crust (Moore, 1981; Peck, 1986). Birnessite  $[(\text{Na},\text{Ca})_{0.5}(\text{Mn}^{4+},\text{Mn}^{3+})_2\text{O}_4 \cdot 1.5\text{H}_2\text{O}]$  is the most common manganese mineral in caves (e.g., Bosák *et al.*, 2002). Other minerals containing Mn found

in caves are chalcophanite  $[\text{ZnMn}^{4+}_3\text{O}_7 \cdot 3\text{H}_2\text{O}]$ , cryptomelane  $[\text{K}(\text{Mn}^{4+},\text{Mn}^{3+})\text{O}_{16}]$ , hausmannite  $[\text{Mn}^{2+}\text{Mn}^{3+}_2\text{O}_4]$ , pyrolusite  $[\text{Mn}^{4+}\text{O}_2]$ , rancieite  $[(\text{Ca},\text{Mn}^{2+})_{0.2}(\text{Mn}^{4+},\text{Mn}^{3+})\text{O}_2 \cdot 0.6\text{H}_2\text{O}]$ , romanechite  $[(\text{Ba},\text{H}_2\text{O})_2(\text{Mn}^{4+},\text{Mn}^{3+})_5\text{O}_{10}]$  and todorokite  $[(\text{Na},\text{Ca},\text{K},\text{Ba},\text{Sr})(\text{Mn},\text{Mg},\text{Al})_6\text{O}_{12} \cdot 3\text{H}_2\text{O}]$  (Peck, 1986; Hill and Forti, 1997; White *et al.*, 2009). Bernardini *et al.* (2021) studied manganese patinas with stromatolite-like features in Del Cervo Cave (Italy). Manganese deposits could be enriched in a spectrum of trace elements and rare-earth elements, such as Ni, Co, P and/or other heavy and trace elements that are associated with Mn-bearing deposits (e.g., Bosák *et al.*, 2002). The origin of manganese minerals deposited in caves is often described as being the result of microbial activity (Peck, 1986; Northup and Lavoie, 2001). They also occur in flowstones as amorphous manganese oxides (Gradziński *et al.*, 1995; Hill and Forti, 1997).

Host rocks and allogenic clastic material, transported into caves by water, could be the source of Mn compounds as well. It should be noted that the identification of manganese

oxides occurring in caves is usually difficult, owing to the poor crystallinity of the minerals (Moore, 1981; Kashima, 1983).

Although the occurrence of manganese deposits in caves is quite common, manganese pebbles are not often found there. There is an almost complete lack of studies of this type of cave sediment, either autogenic or allogenic. Bosák *et al.* (1999) described small concretions transported into the cave from eroded soils of *terra rossa* type. Massive, hard, autogenic Mn-oxide concretions were described in the Bohemian Karst by Čílek and Fábry (1989).

This paper describes one of the first studies, carried out in caves in the central part of the Hoher Göll Massif (cf. Kicińska, 2021; Szczygieł *et al.*, 2022). It presents the possibility of palaeogeographic reconstruction, based on clastic sediments and their mineralogy, as in earlier speleological studies, carried out in the eastern part of the massif (Klappacher and Knapczyk, 1979).

This paper deals with the unique manganese pebbles found in the Hochschartehöhlesystem Cave, their basic mineralogical characteristics, and their genesis and provenance. This is the first description of manganese deposits of this type, found in a cave.

## GEOLOGICAL AND GEOMORPHOLOGICAL SETTING

The Hoher Göll Massif is located ca 20 km south of Salzburg City (Fig. 1) along the Austrian-German border as a part of the Berchtesgaden Alps. The altitude difference between the highest peak (Hoher Göll, 2,522 m a.s.l.) and the bottom of the valleys reaches 2,000 m. The Massif extends in a W–E direction and is ~3 km wide and ~11 km long. The Hoher Göll Massif is limited by the Salzach Valley in the east, the Bluntautal Valley in the south, the Königssee

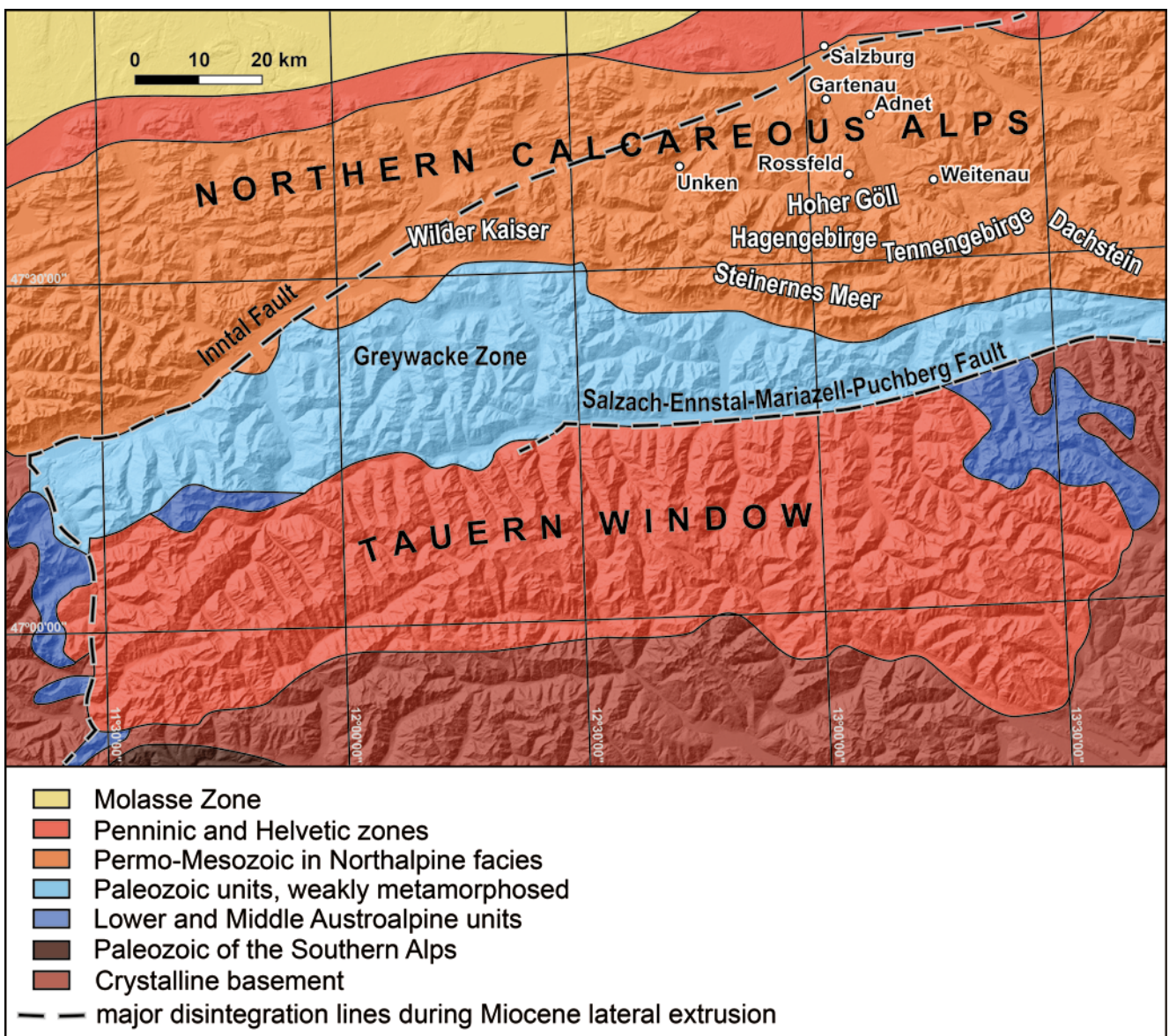


**Fig. 1.** Tectonic sketch of the Northern Calcareous Alps with adjacent areas and the discussed locations, after Beck-Mannagetta and Matura (1980) and Frisch and Gawlick (2003), simplified and redrawn.



Lake and Königsseeache River in the west, and the Weissenbachtal Valley in the north. The central and eastern parts of the massif drain into the Schwarzbachfall/Gollinger Wasserfall (Fig. 2). The whole surface of the karst covers an area of ca 25 km<sup>2</sup> (Klappacher and Knapczyk, 1979).

The Hoher Göll Massif belongs to the Austro-Alpine mega-unit of the Eastern Alps (Tollman, 1980). It is composed of Mesozoic rocks, mostly Middle and Upper Triassic carbonates (Fig. 2) with Jurassic limestones and radiolarites in the north and the west (Plöchinger, 1955, 1987; Braun, 1998). The main ridge is made up of the Dachstein Limestone, underlain by the Wetterstein Dolomite, the Ramsau Dolomite, and the Ramsau/Reifling Limestone (Plöchinger, 1987; Braun, 1998).

The Hoher Göll is one of the smallest massifs in the Berchtesgaden Alps, without extensive plateaus like those in the Tennengebirge and Hagengebirge massifs. Most of the caves are developed in the Upper Triassic Dachstein

Limestone, 2–3 km thick (Zankl, 1969). Currently, 352 caves are known and registered in the cave cadastre in the Massif (Landesverein für Höhlenkunde, Speleological Club, Salzburg), including the Hochschartehöhlesystem and Jubiläumsschacht caves, the depths of which exceed 1,000 m (Klappacher and Völkl, 2016). The caves here, as in other massifs of the Northern Calcareous Alps, belong to the Ruin (ca. 2,000 ± 300 m a.s.l.), Giant (ca 1,600 ± 500 m a.s.l.) and Spring (ca. ~800 ± 300 m a.s.l.) cave levels (Fig. 3; Fischer, 1990; Frisch *et al.*, 2001). The caves trap and preserve various clastic sediments that were transported by rivers or waters, flowing from melting glaciers and seasonal snow fields. The sediments accumulate in sumps and passage bottoms. Such cave clastics can be transported into the caves many times within the underground drainage system or washed out of the caves (e.g., Zupan Hajna *et al.*, 2008). Nevertheless, the remains of such mixed sediments are often found, especially in Alpine karsts.

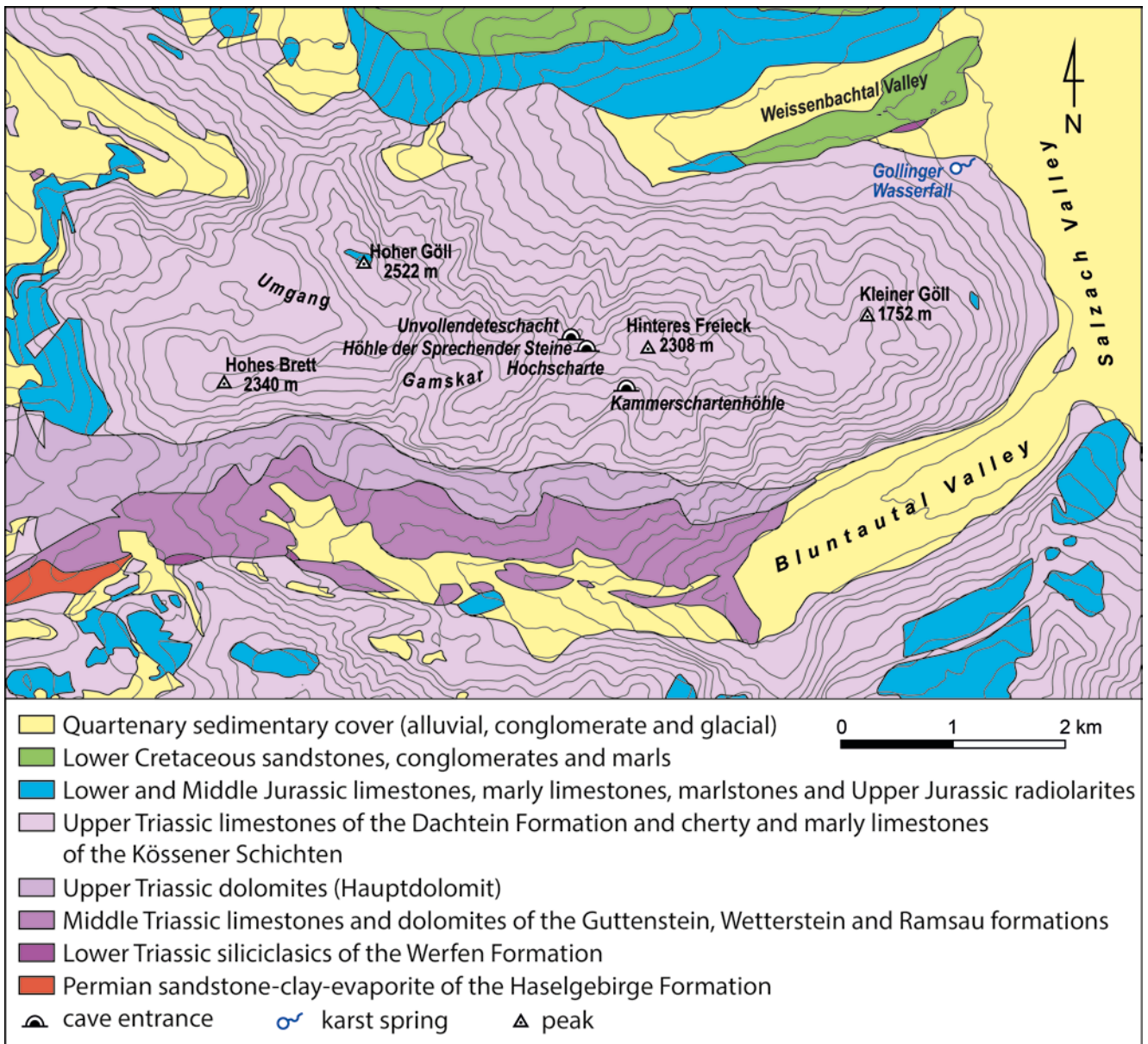


**Fig. 2.** Geological map of the Hoher Göll Massif with location of studied cave system, simplified and modified after Tichy *et al.* (1979) and Plöchinger (1987).

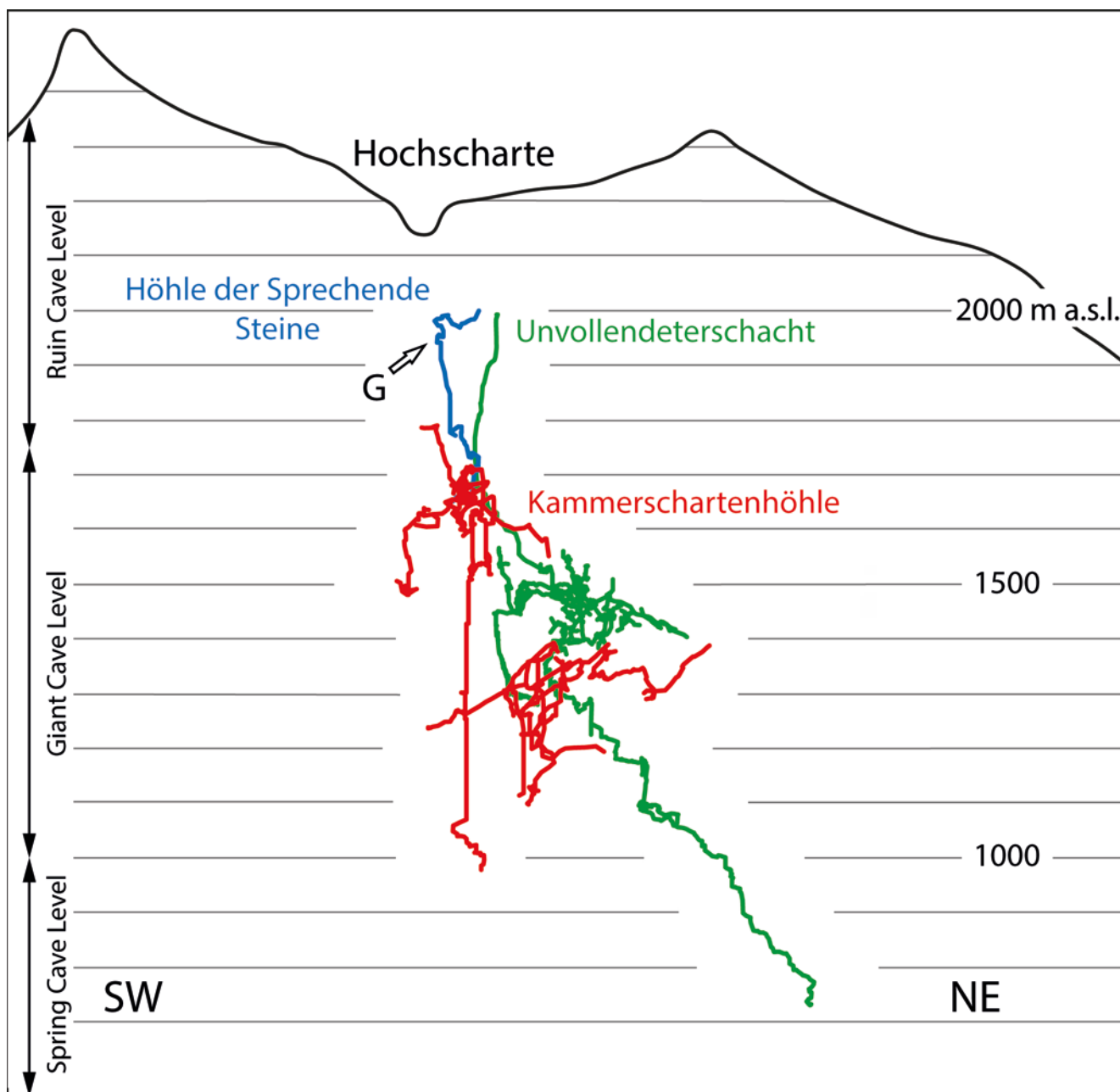


Fig. 3. Schematic cross-section of the Hochschartehöhlensystem with sampling site of clastic deposits.

The research was carried out in the Hochschartehöhlensystem Cave in the central part of the Hoher Göll Massif (Fig. 2). The system consists of four caves, interconnected by cave exploration activities: Höhle der Sprechender Steine, Engstellenschacht, Kammerschartenhöhle and Unvollendeteschacht (Fig. 3). The total length of the system is 14,668 m, and the vertical extent is 1,394 m (Golicz, 2013).

## MATERIALS AND METHODS

Cave clastic sediments were collected from the Site G, which is located in the upper parts of the Höhle der Sprechender Steine (part of the Hochschartehöhlensystem; G, Fig. 3), where a large number of black and heavy pebbles,

mixed with sands and gravels, were found. These sediments, discussed in the paper, chaotically covered a collapse, located in the upper part of the deep pit and part of the wall above it. Among dozens of pebbles, six pebbles were selected for laboratory testing and marked G1–G6 (Fig. 4).

Samples taken from each pebble were subjected to X-ray diffraction (XRD), using a Thermo Electron ARL X'tra diffractometer based on a vertical  $\theta$ - $\theta$  Bragg-Brentano geometry, with  $\text{CuK}\alpha$  radiation, equipped with a solid state Si(Li) detector. The following parameters were applied to the measurements: voltage 40 kV, amperage 30 mA, and power 1200 W. The range of measurements in continuous scan mode was from  $20^\circ$  to  $70^\circ$   $2\theta$ , with a step size of  $0.02^\circ$  per second.

Thin sections of the pebbles (G1, G2, G3 and G4) were made and examined in an Olympus AX70 Provis



petrographic microscope using reflected light. Differential interference contrast (DIC) was used to highlight the surface morphology.

Further investigations of texture and morphology were carried out with a Hitachi S-3700N scanning electron microscope (SEM) in back-scattered (BSE) and secondary electron (SE) modes. The chemical composition in microareas was detected with an energy dispersive spectrometer (EDS) Noran SIX. Analyses were performed in the Institute of Geology of the Faculty of Geographical and Geological Sciences (the Adam Mickiewicz University, Poznań, Poland).

## RESULTS

The pebbles selected for the study varied both in size and weight. The largest one has a diameter of 5.5 cm (380 g), while smaller pebbles with diameters of 1–2 cm and correspondingly lower weights of around 6–10 g predominated. All the specimens are irregular and dome-like, slightly elongated; they have high density and with very shiny black surfaces. Even at the macroscopic level, samples G1, G2 and G6 have a granular texture and massive structure (Fig. 4).

### XRD analysis

The results of mineral composition of pebbles are presented in Table 1. In all samples, the major phase is braunite  $[\text{Mn}^{2+}\text{Mn}^{3+}_6(\text{SiO}_4)_8\text{O}_8]$  with the main  $2\theta$  reflections: 33.04; 38.22; 55.4 degrees (Fig. 5). In samples G1, G2, G4 and G5, peaks observed with  $2\theta$  values of 28.7; 37.4; 56.7 degrees may represent pyrolusite or hollandite  $[\text{Ba}(\text{Mn}^{4+}_6\text{Mn}^{3+}_2)\text{O}_{16}]$ . The presence of hollandite is supported by two  $2\theta$  peaks: 28.7 and 37.4 degrees; but no other reflections typical for this mineral. In the G3 sample (Fig. 5C), besides braunite, diasporite  $[\text{AlO}(\text{OH})]$  is present – a mineral associated with laterite weathering.

### Optical microscopy, SEM-EDS analysis

Thin sections of samples G1 (largest pebble), G2 and G3 revealed the presence of biogenic-like colloform textures (Fig. 6A–C). In sample G4, the laminar texture is less distinct (although discernible), which may stem from the intersection of the cross-section or the degree of crystallization of the mineral phases (Fig. 6D). The dominant pattern is an alternating arrangement of light, massive laminae with convex relief and dark laminae with concave relief and irregular morphology.

The laminae with a convex relief are composed of two mineral phases, differing in colour and birefractance (Fig. 7A). In plane-polarized light (PPL), the light grey phase is clearly dominant, showing very weak pleochroism and anisotropy. In cross-polarized light (XPL), it is dark grey with a brown shade (Fig. 7B). The light grey phase forms a dominant cement, which replaces the creamy-white phase. The creamy-white phase forms a relict type of texture. Pleochroism of the creamy-white phase is not noticeable, while in XPL the authors obtained clear anisotropy and a metallic-grey colour.

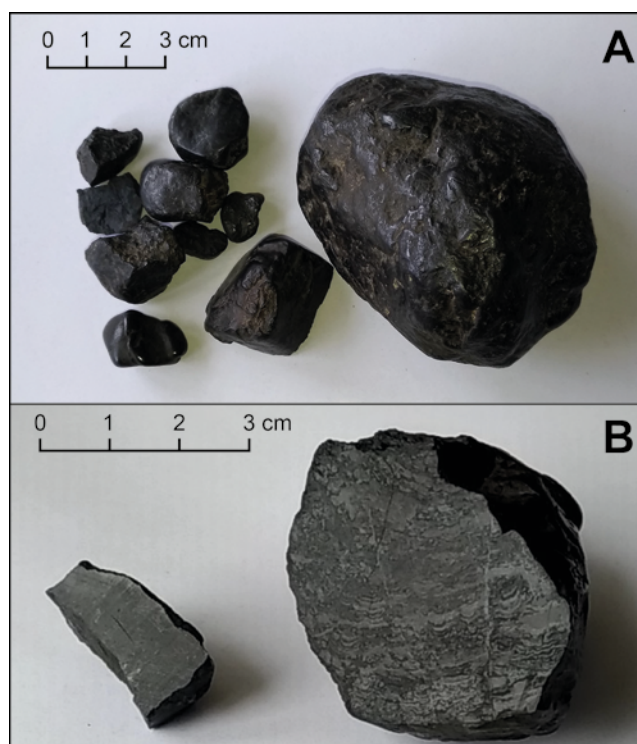


**Fig. 4.** Samples of analysed braunite nodules from the Hochschartehöhlesystem (A) and cross-section of G1 sample (concretion) with visible a stromatolite-like texture (B).

**Table 1**

Mineral composition of pebbles determined by XRD.

	G1	G2	G3	G4	G5	G6
braunite	+	+	+	+	+	+
pyrolusite	+/-	-	-	-	+/-	-
hollandite	+/-	-	-	-	+/-	+/-
diasporite	-	-	+	-	-	-

The SEM-BSE images confirm the presence of two separate mineral phases, differing in density (Fig. 8A, B). Dark grey, less dense areas, composed of Mn and Si show the presence of braunite (Fig. 8A). Braunite is often in the form of automorphic crystals. Due to the Ca admixture, it may be a form of braunite-II (not confirmed by XRD). Creamy white, denser areas are formed by Mn and Ba, which indicate the presence of hollandite (Fig. 8B).

The laminae with concave relief have irregular morphology, related to the presence of a number of scattered fine-spherical particles, resembling accumulations of biogenic mats (Fig. 9A, B). Within them, the authors found fine and coarse braunite, which is undoubtedly secondary after a biogenic-like texture (Fig. 10A). Chemically, they are enriched in Mn (sample G1; Fig. 10B) or enriched in Fe (sample G1; Fig. 11). The needles of cryptomelane were observed in the near-surface zone of pebble G6. However, it should be considered as secondary (Fig. 12). The total

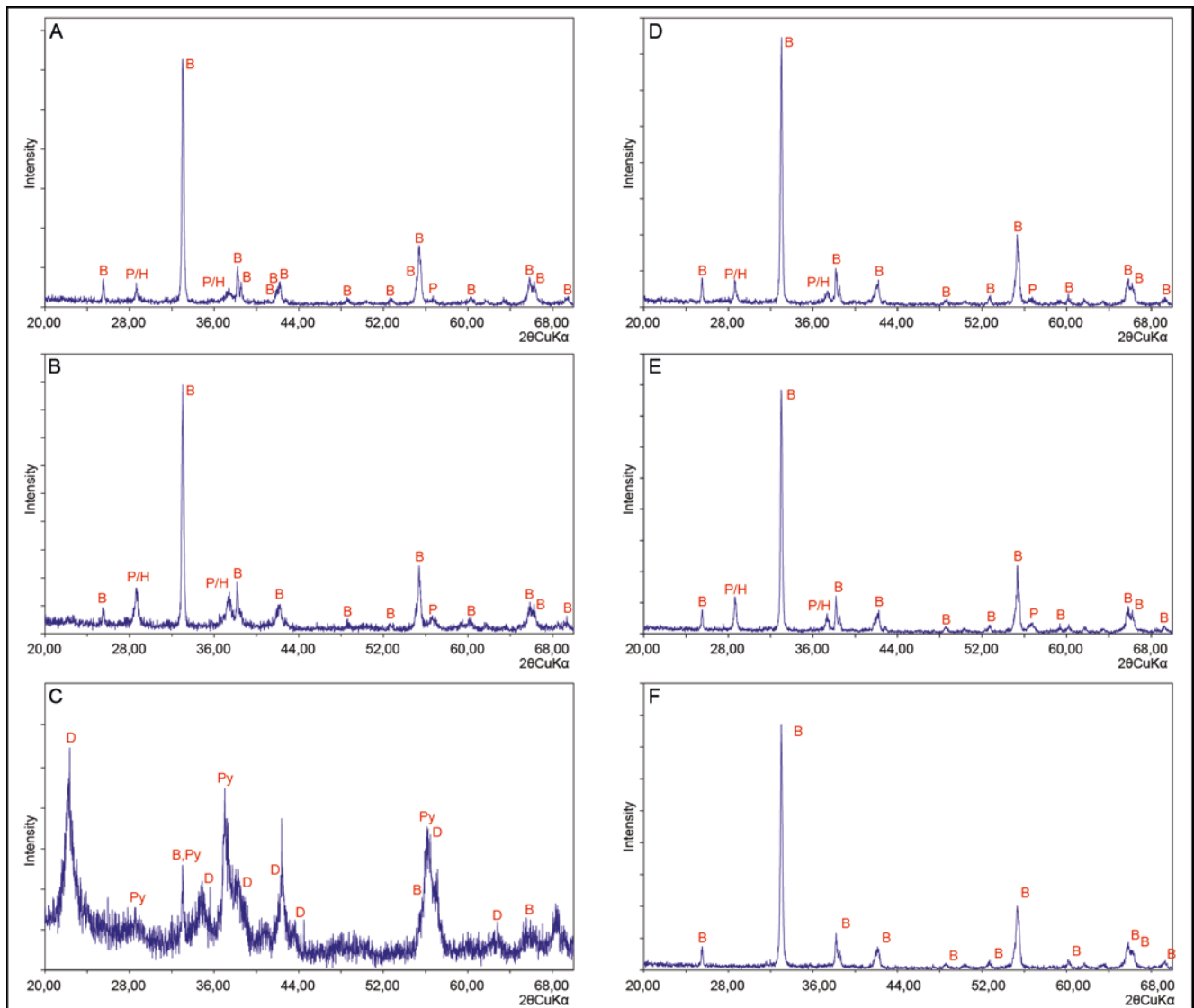


**Fig. 5.** XRD patterns of Mn pebble samples. **A.** G1. **B.** G2. **C.** G3. **D.** G4. **E.** G5. **F.** G6. Abbreviations: B – braunite, P/H – pyrolusite or hollandite, D – diaspore, Py – pyrite.

**Table 2**

Semi-quantitative chemical composition obtained by SEM-EDS analysis of specimens G1–G4.

	G1	G2	G3	G4
	[wt. %]			
O	25.99S	26.00S	25.43S	24.53S
Mg	0.06	0.00	0.00	0.00
Al	0.93	0.93	0.44	0.67
Si	3.83	3.29	3.37	2.85
K	0.34	0.58	0.07	0.32
Ca	1.14	1.39	1.04	1.06
Mn	59.84	58.41	59.99	68.27
Fe	5.96	8.44	7.88	0.77
Ba	1.90	0.95	1.77	1.53

semi-quantitative chemical composition of nodules G1, G2, G3 and G4 determined by scanning an area of approximately 15 mm<sup>2</sup>, is presented in Table 2.

Consistent results from petrographic and SEM-EDS analyses indicate that the dominant component of the pebbles is manganese silicate (braunite). The results of the chemical composition are consistent with those of the petrographic studies, also showing the presence of manganese and barium oxides as quantitatively the second component of the pebbles studied. Despite the ambiguity of the XRD analyses, the authors assume that the second mineral phase is hollandite, formed at higher, hydrothermal temperatures (cf. Hansel and Lehrman, 2016). All pebbles studied are characterized by the presence of biogenic mats, resembling a stromatolite-like texture. Manganese is by far the dominant element, while the Fe content is approximately 10 times lower.



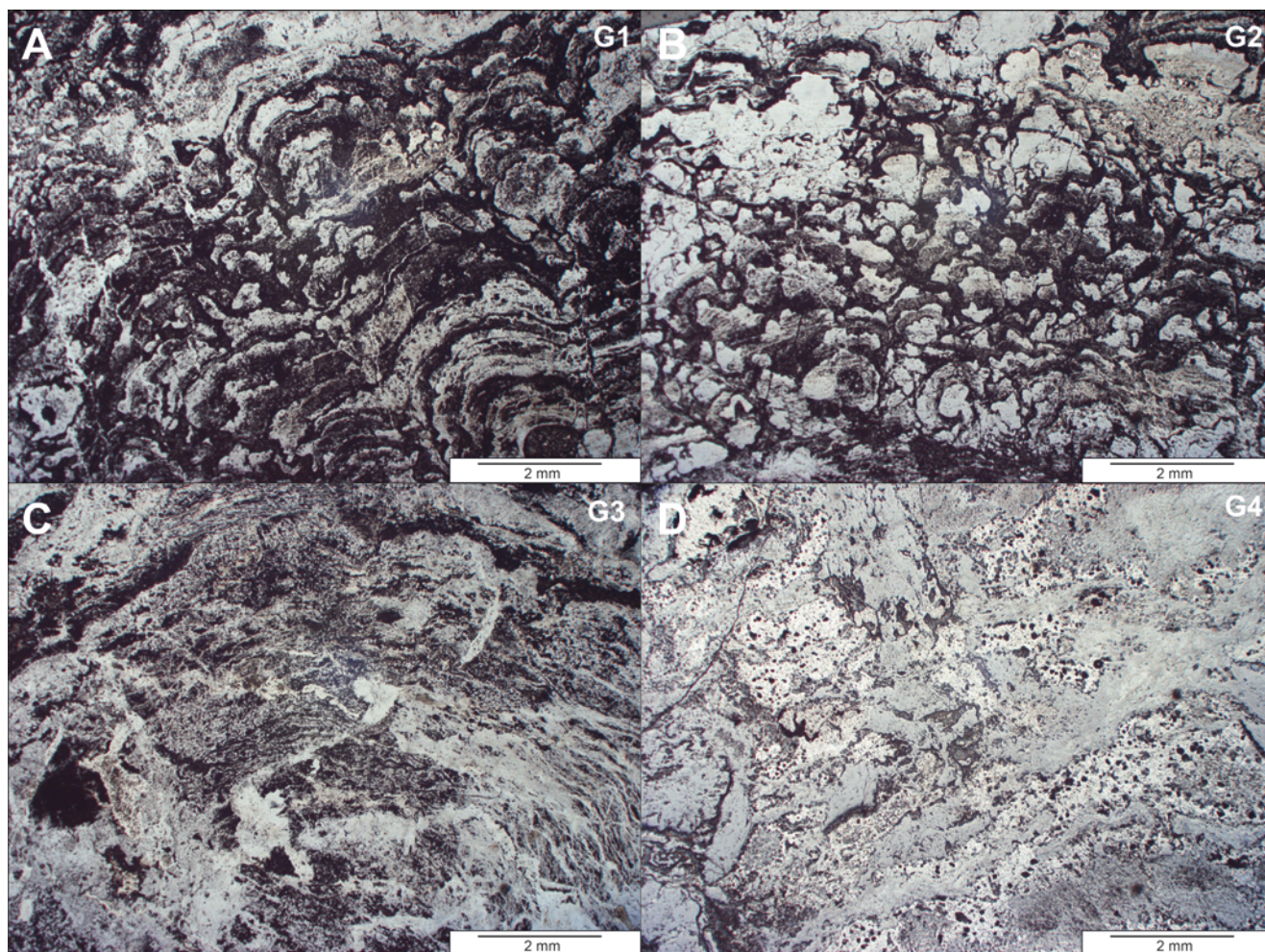


**Fig. 6** Microscopic view of thin sections samples in reflected light (PPL). **A.** G1. **B.** G2. **C.** G3. **D.** G4.

## DISCUSSION

The analysed Mn-rich pebbles were formed outside the caves; they represent allogenic, redeposited material. Their moderate roundedness indicates rather a short transport distance from local sources. They were formed on the surface or come from older eroded rocks.

In the literature on the Northern Calcareous Alps caves, descriptions of clastic sediments similar to the manganese pebbles studied are known. The vast majority of these are iron oxides, originating as weathered material of the Augenstein Formation. Siliciclastic sediments were deposited on the Dachstein palaeo-surface from the Oligocene to the Miocene (Frisch *et al.*, 2001). Later, as the mountains were uplifted, the weathered material was eroded and transported from the surface to the caves by allogenic streams (Frisch *et al.*, 2001; Audra *et al.*, 2002; Clemens *et al.*, 1995; Häuselmann *et al.*, 2020; Kicińska, 2021). In the macroscopic image, some of these sediments are very similar to manganese pebbles. However, the lack of manganese deposits in this part of the Alps excludes this region as a source area. It seems unlikely that it could be a product of weathering of the Augenstein Formation rocks.

Giving consideration to the above facts, it is most probable the manganese pebbles come from eroded Mesozoic rocks.

Manganese mineralization in the Northern Calcareous Alps took place the late Pliensbachian, the late Toarcian to middle Aalenian, the early to middle Bathonian and the Oxfordian (Cornelius and Plöchinger, 1952; Plöchinger, 1955; Jurgan, 1968; Germann, 1973; Jenkyns *et al.*, 1991; Krainer *et al.*, 1994; Ebli *et al.*, 1998). It is worth noting that the greatest amount of Jurassic manganese mineralization is associated with the Upper Liassic marls and shales (“manganese shales”, “Manganschiefer”) extending over a length of 250 km from the west to the east of the Northern Calcareous Alps (Germann, 1973). Many authors attribute the increased Mn content in the Jurassic period to volcanism and progressive rifting of the Tethys passive continental margin (Corbin *et al.*, 2000; Sabatino *et al.*, 2009). Studies of manganese deposits from Late Jurassic Tennenengebirge strata and Early Jurassic strata of the Karwendel Mts, on the basis of rare earth, major and trace elements indicated their hydrothermal and hydrogenous origins (Rantitsch *et al.*, 2003).

While Mn mineralization is common in the Tethys Jurassic, the occurrence of braunite is rare. In the Northern Calcareous Alps, braunite has been found only in a few places, such as the upper Liassic marls and shales in the western part of the Steinernes Meer Massif (Germann, 1973; Günther and Tichy, 1979) and the Tennenengebirge Massif (Cornelius and Plöchinger, 1952). Germann (1973)



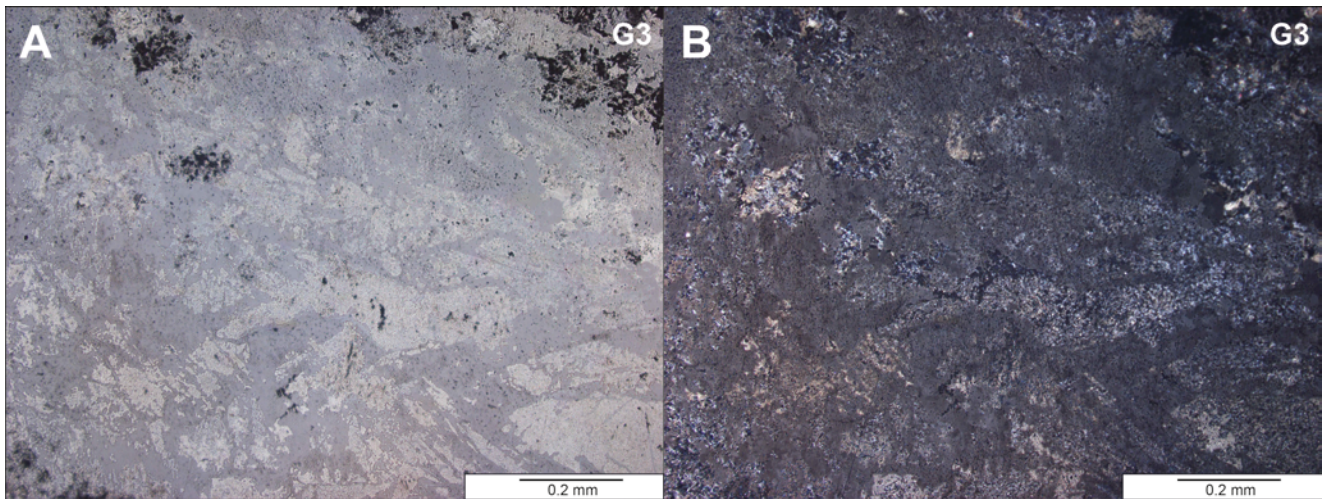


**Fig. 7.** Micrograph of sample G3 in reflected light. **A.** PPL. **B.** XPL.

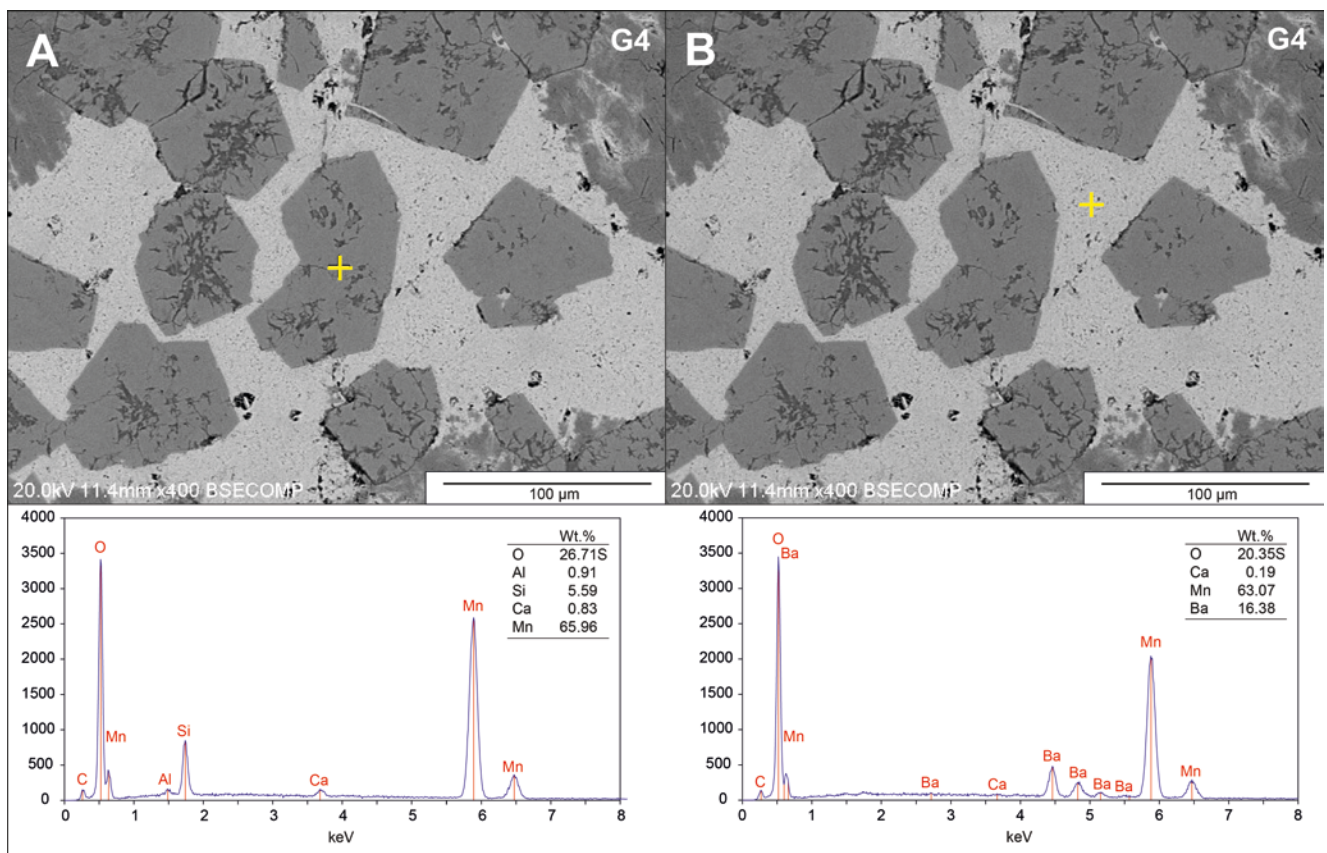


**Fig. 8.** SEM-BSE images of sample G4 with EDS analyses obtained at the point highlighted by the cross. **A.** Polygonal braunite crystal, **B.** Ba-rich cement.

attributed the formation of braunite as being due to volcanic processes on the basis of the presence of a tuff interbedded with manganese deposits. Loosely lying nodules of braunite, pyrolusite and chalcophanit from the Gamskar cirque were described by Meixner and Paar (1977). This post-glacial cirque is located in the Hoher Göll Massif to the west of the studied cave system. These authors suggested different origins of these deposits (volcanic and metamorphic processes) at different times. Nowadays, these sediments are

not found outcropping in the Hoher Göll Massif. It should be added that the sparse occurrence of braunite in the Tethys Realm, apart from the Northern Calcareous Alps, were stated in the Western Alps (Tumiati *et al.*, 2010) and in the Tatra Mts, i.e., in the Carpathian part of the Tethys Ocean (Jach and Dudek, 2005).

It is worth noting that the presence of braunite is regarded as an indicator of hydrothermal activity, in tectonically active zones, in mid-ocean ridges in particular, or as the



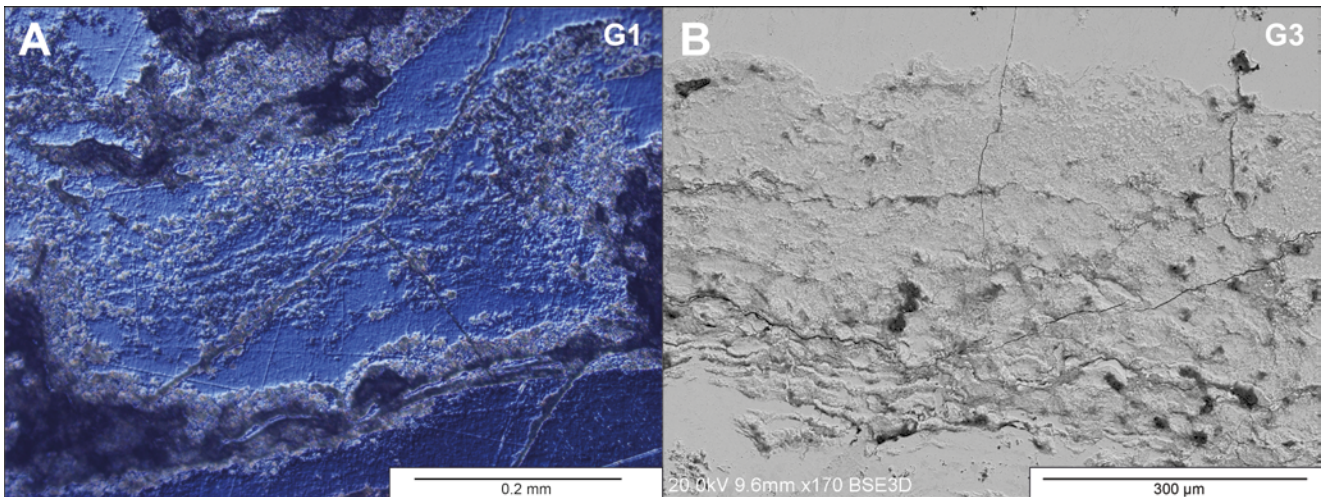


**Fig. 9.** Micrograph of the concave surface of sample G1 (A) in reflected light with DIC mode and the SEM-BSE micrograph of sample G3 (B).

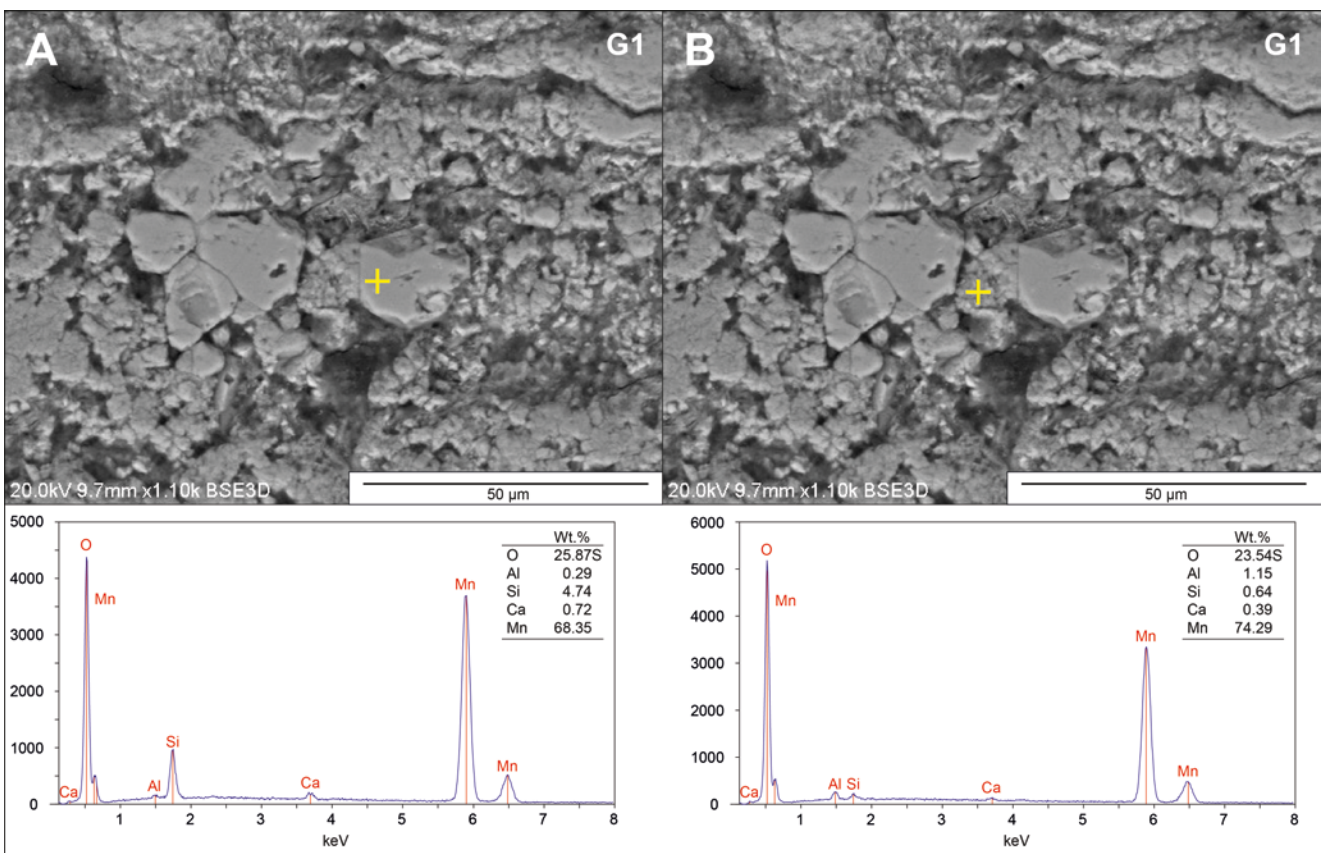


**Fig. 10.** SEM-SE images of sample G1 with EDS analyses obtained at the point highlighted by the cross. **A.** Secondary braunite. **B.** Stromatolite-like matrix

result of depositional-diagenetic processes or very low-grade metamorphism under elevated pressure and temperature (Bonatti *et al.*, 1976; Ostwald, 1992; Roy, 1997; Velilla and Jimenez-Millán, 2003). Thus, the origin of the studied braunite could be related to the occurrence of hydrothermal processes. An additional argument for such a genesis is the fact that the pebbles contain a high content of Si and Ba and a high Mn/Fe ratio, which is observed nowadays in hydrothermal environments (Bonatti *et al.*, 1976; Usui *et al.*, 1997).

It cannot be excluded that studied braunites belong to exotic ophiolites. In the Berchtesgaden Alps, this type of Jurassic rock was discovered by Krische *et al.* (2014) and Gawlick *et al.* (2015). These exotic materials were found in the vicinity of Gartenau, Weitenau and Rossfeld (Fig. 1; Krische *et al.*, 2014), which are adjacent to the study area and several kilometres west of the Hoher Göll Massif (in the vicinity of Unken, Fig. 1; Gawlick *et al.*, 2015). According to Gawlick *et al.* (2015), the first thrusting event related to



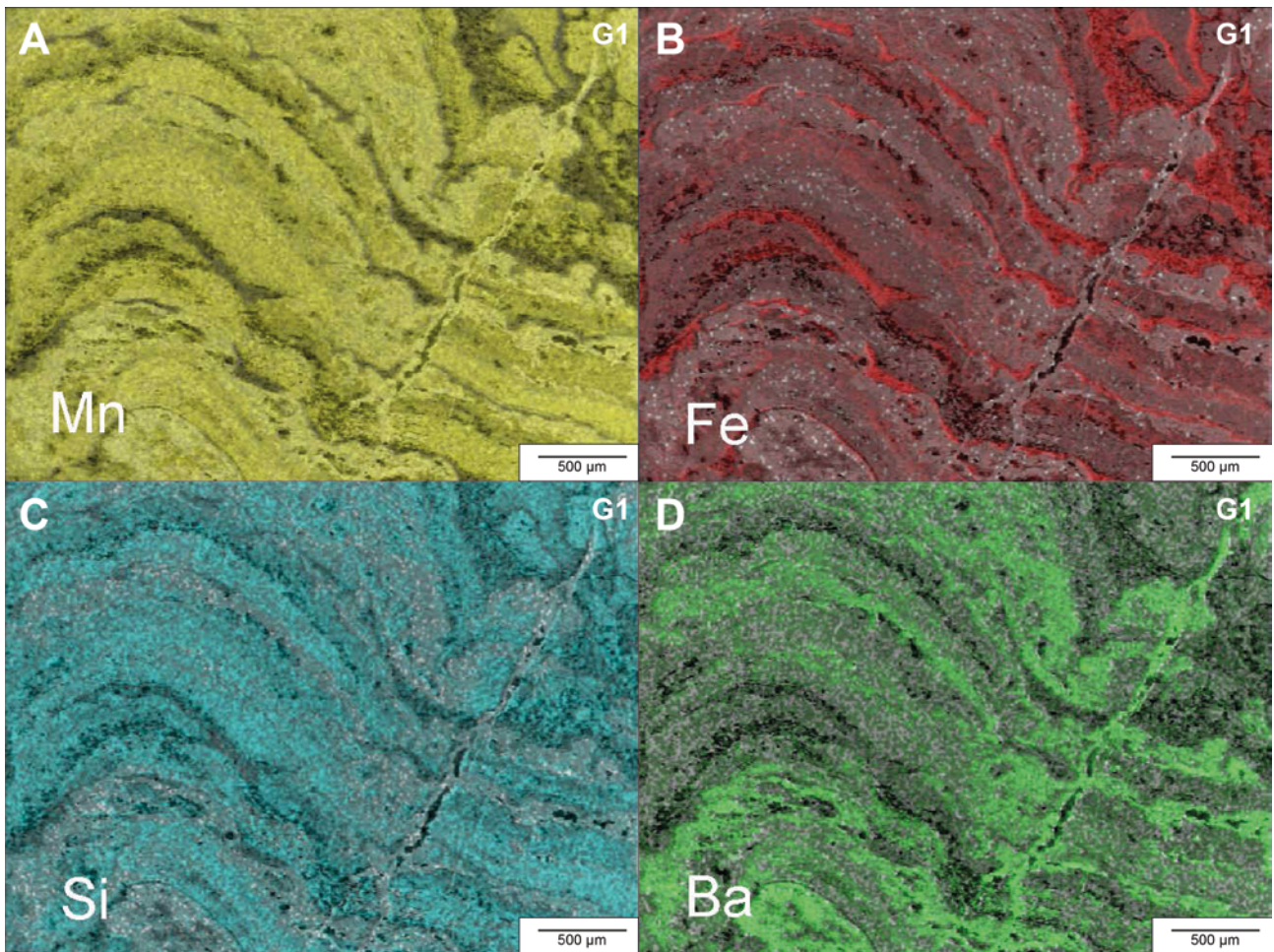
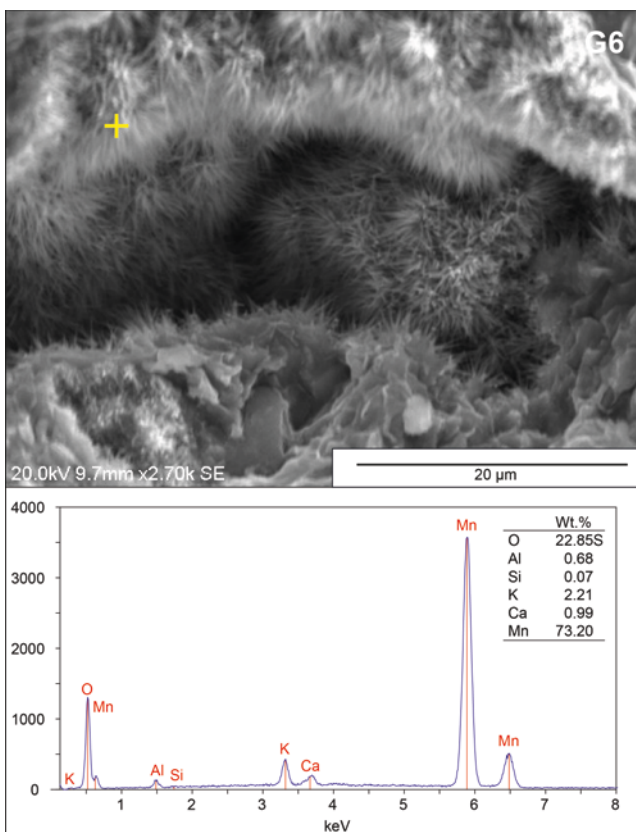


**Fig. 11.** EDS mapping of four main elements for sample G1. The intensity of the color reflects the content of a given element. **A.** Mn. **B.** Fe. **C.** Si. **D.** Ba.



ophiolite obduction (upper plate) in the Northern Calcareous Alps is of Jurassic age, which is under discussion in the Alpine literature.

An important element, indicating the provenance of manganese pebbles, may be the stromatolite-like textures, which, like braunite, were not found *in situ* in the Hoher Göll Massif (cf. Braun, 1988). Nevertheless, in the Upper Triassic Dachstein Limestone of the Höchkönig Massif (massif 20 km south of the study area), there are similar facies, within which both stromatolites and hydrothermal processes have been found (Satterley, 1994). Deep-water stromatolites from the Early and Middle Jurassic near the town of Adnet also are described by Böhm and Brachert (1993).

Taking this into account, there are many possibilities for the origin of the manganese pebbles in the Höhle der Sprechender Steine Cave. Their provenance most likely is related to eroded Jurassic rocks. The Upper Liassic marls and shales (“Manganschiefer”) described by Germann (1973) do not occur in the main ridge of the Hoher Göll Massif, but are located in its western part, in the lower parts of the Hohes Brett Peak slope (Fig. 2; Germann, 1973;

**Fig. 12.** SEM-SE images and EDS spectrum of a Mn phase resembling cryptomelane.



Plöschinger, 1987). It should be emphasized that these Liassic marls and shales are the only rocks of the Berchtesgaden mountains, where braunite has already been found. The largest number of manganese deposits are found in the upper part of the Hochschartehöhle system Cave, a part of the oldest and inactive Ruin Cave Level occurring at ca 2,000 ± 300 m a.s.l. in the Northern Calcareous Alps. This level developed during the Middle Eocene and Early Oligocene (Fischer, 1990; Frisch *et al.*, 2001). The period of water inflow could have been active during late Miocene or even earlier. The cosmogenic-nuclide dating of clastic sediments from the Schaffschacht Cave in the Tennengebirge, the massif adjacent to the study area, shows an age of 6.6 Ma (Häuselmann *et al.*, 2020). By analogy, the material derived from eroded rock could have got into the cave at least before that date (cf. Kicińska, 2021).

## CONCLUSIONS

The pebbles from the upper parts of the Hochschartehöhle system studied are characterized by the presence of braunite, a stromatolite-like internal texture, relatively low Fe, high Si and Ba contents, and high Mn/Fe ratio. Currently, these deposits do not occur *in situ*, owing to surface denudation in the main ridge of the Hoher Göll Massif. The pebbles were derived from local rocks and transported into cave systems after erosion as a part of allogenic cave fills.

Braunite pebbles have never been described in the speleological literature before, either as autogenic or as allogenic deposits. It is a rare record in a cave environment. Its origin could be related to the occurrence of hydrothermal processes. By analogy to modern environments, the genesis of this type of rock could be linked to the spreading zone and the accompanying vents. Undoubtedly, the final solution on the genesis of pebbles requires advanced geochemical analyses.

The occurrence of braunite pebbles in the Hoher Göll Massif is one of the few pieces of evidence indicating the existence of hydrothermal vents in the Northern Calcareous Alps, which is very important for palaeogeographic reconstructions and the regional geology of this area.

## ACKNOWLEDGEMENTS

The authors thank the Landesverein für Höhlenkunde in Salzburg Club (in particular Walter Klappacher and Gerhard Zehntner) and the Department of Nature Conservation in the Federal State Government Salzburg (Amt der Salzburger Landesregierung, Abteilung Naturschutz) for research permission; the colleagues from the clubs (Wielkopolski Klub Tatarnictwa Jaskiniowego in Poznań and Katowicki Klub Speleologiczny in Katowice), who assisted during the field work; Krzysztof Najdek for preparing the figures; Mateusz Golicz and Miłosz Dryjański for providing cave morphometric data; Michał Jankowiak for preparing samples; and Dorota Salata, Michał Gradziński and Julita Biernacka for helpful suggestions. We thank the reviewers Pavel Bosák, Petr Mikysek and Jacek Szczygiel for constructive comments which significantly improved the paper.

## REFERENCES

- Audra, P., Quinif, Y. & Rochette, P., 2002. The genesis of the Tennengebirge karst and caves (Salzburg, Austria). *Journal of Cave and Karst Studies*, 64: 153–164.
- Beck-Mannagetta, P. & Matura, A., 1980. *Geologische Karte von Österreich 1:500 000 – 1 Bl.* Farbdruck, Wien (Geologische Bundesanstalt).
- Bella, P., Gradziński, M., Hercman, H., Leszczyński, S. & Nemeček, W., 2021. Sedimentary anatomy and hydrological record of relic fluvial deposits in a karst cave conduit. *Sedimentology*, 68: 425–448.
- Bernardini, S., Bellatreccia, F., Columbu, A., Vaccarelli, I., Pellegrini, M., Jurado, V., Del Gallo, B., Saiz-Jimenez, C., Sodo, A., Millo, C., Jovane, L. & De Waele, J., 2021. Morpho-mineralogical and bio-geochemical description of cave manganese stromatolite-like patinas (Grotta del Cervo, Central Italy) and hints on their paleohydrological-driven genesis. *Frontiers in Earth Science*, 9: id.692.
- Bonatti, E., Zerbi, M., Kay, R. & Rydell, H., 1976. Metalliferous deposits from the Apennine ophiolites: Mesozoic equivalents of modern deposits from oceanic spreading centers. *Geological Society of America Bulletin*, 87: 83–94.
- Bosák, P., 1989. Clays and sands in paleokarst. In: Bosák, P., Ford, D. C., Glazek, J. & Horáček, I. (eds), *Paleokarst, A Systematic and Regional Review*. Akademia, Praha – Elsevier, Amsterdam, pp. 431–442.
- Bosák, P., Bella, P., Čílek, V., Ford, D. C., Hercman, H., Kadlec, J., Osborne, A. & Pruner, P., 2002. Ochtiná Aragonite Cave (Western Carpathians, Slovakia): morphology, mineralogy of the fill and genesis. *Geologica Carpathica*, 53: 399–410.
- Bosák, P., Mihevc, A., Pruner, P., Melka, K., Venhodová, D. & Langrová, A., 1999. Cave fill in the Črnotiče Quarry, SW Slovenia: palaeomagnetic, mineralogical and geochemical study. *Acta Carsologica*, 28/2: 15–39.
- Boston, P., 2004. Biofilms. In: Gunn, J. (ed.), *Encyclopedia of Caves and Karst Science*. Taylor and Francis Group, New York, pp. 299–303.
- Böhm, F. & Brachert, T. C., 1993. Deep-water stromatolites and *Fruites* Maslov from the Early and Middle Jurassic of S-Germany and Austria. *Facies*, 28: 145–168.
- Braun, R., 1998. *Die Geologie des Hohen Gölls. Torrener-Joch-Zone/Jenner/Hoher Göll eine durch Kontinent/Kontinent-Kollision ausgelöste Gleitdecke in den auglbodenschichten (mittlerer Oberjura) der Berchtesgadener Alpen*. Nationalpark Berchtesgaden, Forschungsbericht 40, Plenk, Berchtesgaden, 192 pp.
- Čílek, V. & Fábry, J., 1989. Epigenetic manganese-rich layers in karst fillings of the Zlatý kůň Hillock, Bohemian Karst. *Československý kras*, 40: 37–55. [In Czech, with English summary.]
- Clemens, T., Jantschke, H. & Schäffler M., 1995. Zur Herkunft der Eisen-Mangan-Erze in Höhlensedimenten der Horizontalhöhlen in der Reiteralme (Berchtesgadener Alpen). *Die Höhle*, 46: 66–74.
- Corbin, J. C., Person, A., Iatzioura, A., Ferré, B. & Renard, M., 2000. Manganese in Pelagic carbonates: indication of major Tectonic events during the geodynamic evolution of a passive continental margin (the Jurassic European Margin of the

- Tethys–Ligurian Sea). *Palaeogeography, Palaeoclimatology, Palaeoecology*, 156: 123–138.
- Cornelius, H. P. & Plöschinger, B., 1952. Der Tennengebirgs-N-Ränd mit seinen Manganerzen und die Berge im Bereich des Lammertales. *Jahrbuch Geologische Bundesanstalt*, 95: 145–225.
- Ebli, O., Vetö, I., Lobitzer, H., Sajgó, C., Demény, A. & Hetényi, M., 1998. Primary productivity and early diagenesis in the Toarcian Tethys on the example of the Mn-rich black shales of the Sachrang Formation, Northern Calcareous Alps. *Organic Geochemistry*, 29: 1635–1647.
- Fischer, K., 1990. Höhlenniveaus und Altreliefgenerationen in den Berchtesgadener Alpen. *Mitteilungen der Geographischen Gesellschaft in München*, 75: 47–59.
- Ford, D. C. & Williams, P. W., 2007. *Karst Hydrogeology and Geomorphology*. Wiley, Chichester, 562 pp.
- Frisch, W. & Gawlick, H.-J., 2003. The nappe structure of the central Northern Calcareous Alps and its disintegration during Miocene tectonic extrusion – a contribution to understanding the orogenic evolution of the Eastern Alps. *International Journal of Earth Sciences*, 92:712–727.
- Frisch, W., Kuhlemann, J., Dunkl, I. & Székely, B., 2001. The Dachstein paleosurface and the Augenstein Formation in the Northern Calcareous Alps – a mosaic stone in the geomorphological evolution of the Eastern Alps. *International Journal of Earth Sciences*, 90: 500–518.
- Gawlick, J. H., Aubrecht, R., Schlagintweit, F., Missoni, S. & Plašienka, D., 2015. Ophiolitic detritus in Kimmeridgian resedimented limestones and its provenance from an eroded obducted ophiolitic nappe stack south of the Northern Calcareous Alps (Austria). *Geologica Carpathica*, 66: 473–487.
- Germann, K., 1973. Deposition of manganese and iron carbonates and silicates in Liassic marls of the Northern Limestone Alps (Kalkalpen). In: Amstutz, G. C. & Bernard, A. J. (eds), *Ores in Sediments*. Springer, Berlin, pp. 129–138.
- Golicz, M., 2013. Recent activity in Hoher Göll. In: Kicińska D. (ed.), *Polish Caving 2009–2013*. Komisja Tatarnictwa Jaskiniowego Polskiego Związku Alpinizmu (Caving Commission of Polish Mountaineering Association). Pracownia Kreatywna Bezliku, Kraków, pp. 13–14.
- Gradziński, M., Banaś, M. & Uchman, A., 1995. Biogenic origin of manganese flowstones from Jaskinia Czarna Cave, Tatra Mts., Western Carpathians. *Annales Societatis Geologorum Poloniae*, 65: 19–27.
- Günther, W. & Tichy, G., 1979. Manganberg- und -schurfbaue im Bundesland Salzburg. *Mitteilungen der Gesellschaft für Salzburger Landeskunde*, 119: 351–373.
- Hansel, C. M. & Learman, D. R., 2016. Geomicrobiology of manganese. In: Ehrlich, H. L., Newman, D. K. & Kappler, A. (eds), *Ehrlich's Geomicrobiology. Sixth Edition*. CRC Press, pp. 403–433.
- Häuselmann, Ph., Plan., L., Pointner, P. & Fiebig, M., 2020. Cosmogenic nuclide dating of cave sediments in the Eastern Alps and implications for erosion rates. *International Journal of Speleology*, 49: 107–118.
- Hercman, H., 2000. Reconstruction of paleoclimatic changes in central Europe between 10 and 200 thousand years BP, based on analysis of growth frequency of speleothems. *Studia Quaternaria*, 17: 35–70.
- Hill, C. A. & Forti, P., 1997. *Cave Minerals of the World*. National Speleological Society, Huntsville, 463 pp.
- Jach, R. & Dudek, T., 2005. Origin of a Toarcian manganese carbonate/silicate deposit from the Křižna unit, Tatra Mountains, Poland. *Chemical Geology*, 224: 136–152.
- Jenkyns, H. C., Géczy, B. & Marshall, J. D., 1991. Jurassic manganese carbonates of Central Europe and the Early Toarcian anoxic event. *Journal of Geology*, 99: 137–149.
- Jurgan, H., 1968. Sedimentologie des Lias der Berchtesgadener Kalkalpen. *Geologische Rundschau*, 58: 464–501.
- Kashima, N., 1983. On the wad-minerals from the cavern environment. *International Journal of Speleology*, 13: 67–72.
- Kicińska, D., 2021. Origin of fine-grained clastic sediments in caves of the Hoher Göll massif (Northern Calcareous Alps, Austria). *Annales Societatis Geologorum Poloniae*, 91: 363–373.
- Klappacher, W. & Knapczyk, H., 1979. *Salzburger Höhlenbuch*. Landesverein für Höhlenkunde in Salzburg, Salzburg, 487 pp.
- Klappacher, W. & Völkl, G., 2016. Hoher Göll. In: Spötl, Ch., Plan, L. & Christian, E. (eds), *Höhlen und Karst in Österreich*. Oberösterreichisches Landesmuseum, Linz, pp. 531–530.
- Krainer, K., Mostler, H. & Haditsch, J. G., 1994. Jurassische Beckenbildung in den Nördlichen Kalkalpen bei Lofer (Salzburg) unter besonderer Berücksichtigung der Manganerzgenese. *Abhandlungen der Geologischen Bundesanstalt*, 50: 257–293.
- Krische, O., Goričan, Š. & Gawlick, J. H., 2014. Erosion of a Jurassic ophiolitic nappe-stack as indicated by exotic components in the Lower Cretaceous Rossfeld Formation of the Northern Calcareous Alps (Austria). *Geologica Carpathica*, 65: 3–24.
- Meixner, H. & Paar, W., 1977. Eine Manganvererzung mit Braunit vom Gamskar am Hohen Göll, Salzburg. *Der Karinthin*, 76: 303–309.
- Moore, G. W., 1981. Origin of black deposits in caves. In: Beck, B. F. (ed.), *Proceedings of the 8th International Congress of Speleology: Bowling Green, Kentucky, U.S.A., July 18 to 24, 1981*. National Speleological Society, Huntsville, Alabama, pp. 642–644.
- Northup, D. E. & Lavoie, K. H., 2001. Geomicrobiology of caves: A review. *Geomicrobiology Journal*, 18: 199–222.
- Ostwald, J., 1992. Mineralogy, paragenesis and genesis of the braunite deposits of the Mary Valley Manganese Belt, Queensland, Australia. *Mineralium Deposita*, 27: 326–335.
- Peck, S. B., 1986. Bacterial deposition of iron and manganese oxides in North American caves. *Bulletin of the National Speleological Society*, 48: 26–30.
- Plöschinger, B., 1955. Zur Geologie des Kalkalpenabschnittes vom Torrener Joch zum Ostfuss des Untersberges; die Göllmasse und die Halleiner Halstätter Zone. *Jahrbuch Geologische Bundesanstalt*, 3: 93–144.
- Plöschinger, B., 1987. *Geologische Karte der Republik Österreich 1:50.000, Blatt 94 Hallein*. Geologische Bundesanstalt, Vienna.
- Rantitsch, G., Melcher, F., Meisel, T. & Rainer, T., 2003. Rare earth, major and trace elements in Jurassic manganese shales of the Northern Calcareous Alps: hydrothermal versus hydrogenous origin of stratiform manganese deposits. *Mineralogy and Petrology*, 77: 109–127.

- Roy, S. J., 1997. Genetic diversity of manganese deposition in the terrestrial geological record. In: Nicholson, K., Hein, J. R., Bühn, B. & Dasgupta, S. (eds), *Manganese mineralisation: Geochemistry and Mineralogy of Terrestrial and Marine Deposits*. Geological Society, London, Special Publication, 119: 5–28.
- Sabatino, N., Neri, R., Bellanca, A., Jenkyns, H. C., Masetti, D. & Scopelliti, G., 2009. Petrography and high-resolution geochemical records of Lower Jurassic manganese-rich deposits from Monte Mangart, Julian Alps. *Palaeogeography, Palaeoclimatology, Palaeoecology*, 299: 97–109.
- Sasowsky, I. D., 2007. Clastic sediments in caves – imperfect recorders of processes in karst. *Acta Carsologica*, 36: 143–149.
- Satterley, A. K., 1994. Sedimentology of the Upper Triassic reef complex at the Hochkönig Massif (Northern Calcareous Alps, Austria). *Facies*, 30: 119–149.
- Szczygieł, J., Wróblewski, W., Mendecki, M. J., Hercman, H., & Bosák, P., 2020a. Soft-sediment deformation structures in cave deposits and their possible causes (Kalacka Cave, Tatra Mts., Poland). *Journal of Structural Geology*, 140: 104–161.
- Szczygieł, J., Hercman, H., Hoke, G., Gašiorowski, M., Błaszczuk, M. & Sobczyk, A., 2020b. No valley deepening of the Tatra Mountains (Western Carpathians) during the past 300 ka. *Geology*, 48: 1006–1011.
- Szczygieł, J., Baroň, I., Melichar, R., Plan, L., Mitrović-Woodell, I., Kaminsky, E., Scholz, D. & Grasemann, B., 2022b. Post-Miocene tectonics of the Northern Calcareous Alps. *Scientific Reports*, 12: 17730.
- Tichy, G., 1979. *Geologische Karte der Rossfeldgruppe, des Hohen Göll und des Hagengebirges 1:50 000*. In: Klappacher, W. & Knapczyk, H. (eds), *Salzburger Höhlenbuch*. Landesverein für Höhlenkunde in Salzburg, 3.
- Tollman, A., 1980. Geology and Tectonics of the Eastern Alps (middle sector). *Abhandlungen der Geologischen Bundesanstalt*, 34: 197–255.
- Tumiati, S., Martin, S. & Godard, G., 2010. Hydrothermal origin of manganese in the high-pressure ophiolite metasediments of Praborna ore deposit (Aosta Valley, Western Alps). *European Journal of Mineralogy*, 22: 577–594.
- Usui, A., Bau, M. & Yamazaki, T., 1997. Manganese microchimneys buried in the Central Pacific pelagic sediments: evidence of interpolate water circulation? *Marine Geology*, 141: 269–285.
- Velilla, N. & Jiménez-Millán, J., 2003. Origin and metamorphic evolution of rocks with braunite and pyrophanite from the Iberian Massif (SW Spain). *Mineralogy and Petrology*, 78: 73–91.
- White, W. B., Vito, C. & Scheetz, B. E., 2009. The mineralogy and trace element chemistry of black manganese oxide deposits from caves. *Journal of Cave and Karst Studies*, 71: 136–143.
- Zankl, H., 1969. Der Hohe Göll. Aufbau und Lebensbild eines Dachstein-Riffes in der Obertrias der nördlichen Kalkalpen. *Abhandlungen der Senckenberg Gesellschaft*, 519: 1–120.
- Zupan Hajna, N., Mihevc, A., Pruner, P. & Bosák, P., 2008. Palaeomagnetism and magnetostratigraphy of karst sediments in Slovenia. *Carsologica*, 8: 1–266.



